Image-based Material Editing for Making Reflective Objects Fluorescent

Daichi Hidaka and Takahiro Okabe
Department of Artificial Intelligence, Kyushu Institute of Technology, Japan
okabe@ai.kyutech.ac.jp

Keywords: Image-based Material Editing, Photometric Consistency, Fluorescence, Reflection, Spectral Irradiance.

Abstract: Fluorescent materials give us a unique sense of quality such as self-luminous ones, because they absorb light with certain wavelengths and then emit light with longer wavelengths. The existing methods for image-based material editing make objects in an image specular, translucent, and transparent, but they do not address fluorescent materials. In this paper, we propose a method for making reflective objects in a single input image fluorescent by adding photorealistic fluorescent components to the objects of interest. Specifically, we show that photometrically consistent fluorescent components can approximately be represented by using the 3-band (RGB) spectral irradiance on the surface of a reflective object, and then compute the fluorescent components on the basis of intrinsic image decomposition without explicitly estimating the object's shape and the light sources illuminating it from the input image. We conducted a number of experiments using both synthetic and real images, and confirmed that our proposed method is effective for making reflective objects fluorescent.

1 INTRODUCTION

Fluorescence is a very common phenomenon observed both in natural objects such as minerals and plants and in man-made objects such as papers and clothes (Barnard, 1999). Fluorescent materials absorb light with certain wavelengths and then emit light with longer wavelengths, in contrast to reflective materials which reflect light with the same wavelengths as those of the incident light. Therefore, they give us a unique sense of quality such as self-luminous materials.

Image-based material editing is a technique for automatically and photo-realistically replacing one material in an image with another. Khan *et al.* (Khan et al., 2006) propose a method for making an object in a single input image specular, translucent, and transparent. Since the appearance of an object depends on the shape of the object and the light sources illuminating it, their proposed method roughly estimates the depth map of the object and the illumination distribution of a scene from the input image on the basis of heuristics. Liu *et al.* (Liu et al., 2017) propose an end-to-end network architecture that predicts the shape, illumination, and material from a single image, and make use of the predicted results for material editing of diffuse and specular objects.

On the other hand, fluorescent materials are not addressed in the context of image-based material editing. They are addressed mainly in the context of reflection separation, *i.e.* separating reflective and fluorescent components under narrow-band camera assumption (Zhang and Sato, 2013), under narrow-band illumination assumption (Koyamatsu et al., 2019), and by using high-frequency illumination in the spectral domain (Fu et al., 2016b), and in the context of image-based modeling, *i.e.* recovering the spectral properties of reflection and fluorescence (Fu et al., 2016a).

In this paper, we propose a method for making reflective objects in a single input image fluorescent by adding photorealistic fluorescent components to the objects of interest. Specifically, we show that photometrically consistent fluorescent components can approximately be represented by using the 3-band (RGB) spectral irradiance on the surface of a reflective object. Therefore, our proposed method computes the fluorescent components on the basis of intrinsic image decomposition (Tappen et al., 2005) without explicitly estimating the object's shape and the light sources illuminating it from the input image.

We conducted a number of experiments using both synthetic and real images, and confirmed that the approximation represented by using the 3-band spectral irradiance works well and that our proposed method is effective for making reflective objects fluorescent. The application scenarios of our method include the appearance simulation of fluorescent materials for traffic signs, commercial posters, manufactured products, and so on.

Hidaka, D. and Okabe, T.
Image-based Material Editing for Making Reflective Objects Fluorescent.
In *Proceedings of the 15th International Joint Conference on Computer Vision, Imaging and Computer Graphics Theory and Applications (VISIGRAPP 2020) - Volume 1: GRAPP*, pages 355-360
ISBN: 978-989-758-402-2

The main contributions of this study are twofold. First, based on the fluorescent model, we show that photometrically consistent fluorescent components can approximately be represented by using the 3-band spectral irradiance on the surface of a reflective object. It enables us to compute the fluorescent components on the basis of intrinsic image decomposition without explicitly estimating the object's shape and the light sources illuminating it from an input image. Second, we experimentally confirmed that our proposed method is effective for making reflective objects in a single input image fluorescent. Specifically, we confirmed that the approximation represented by using the 3-band spectral irradiance works well through qualitative and quantitative evaluation using synthetic images, and that our method provides visual enrichment of photographs with virtual fluorescence.

2 PROPOSED METHOD

2.1 Overview

For fluorescent materials, the pixel value $i_b(\boldsymbol{x})$ at a point $\boldsymbol{x}$ on an object surface consists of a reflective component $r_b(\boldsymbol{x})$ and a fluorescent component $f_b(\boldsymbol{x})$ as

$$i_b(\boldsymbol{x}) = r_b(\boldsymbol{x}) + f_b(\boldsymbol{x}), \tag{1}$$

where b $(b = 1,2,3)$ stands for the band (RGB) of a color camera. Our proposed method assumes that an object of interest has only the first term, *i.e.* the reflective component, and then adds the second term, *i.e.* the fluorescent component to the object surface. In this section, we explain the fluorescence model and the diffuse reflection model, and then explain our method for computing photometrically consistent fluorescent components.

2.2 Fluorescence Model

In general, a pure fluorescent material absorbs light with a certain wavelength λ', and then emits light with a longer wavelength λ''. Those properties are described by the absorption spectrum $a(\lambda')$ and the emission spectrum $e(\lambda'')$ (Zhang and Sato, 2013).

When a fluorescent material is illuminated by distant light sources from various directions with various wavelengths, the fluorescent component is given by

$$\begin{aligned} f_b(\boldsymbol{x}) &= \int a(\lambda') \left[\int l(\boldsymbol{\omega},\lambda') \boldsymbol{\omega}^\top \boldsymbol{n}(\boldsymbol{x}) d\boldsymbol{\omega} \right] d\lambda' \\ &\times \int c_b(\lambda'') e(\lambda'') d\lambda''. \end{aligned} \tag{2}$$

Here, $l(\boldsymbol{\omega},\lambda')$ describes the energy of the light rays from the direction $\boldsymbol{\omega}$ and with the wavelength λ', *i.e.* the spectral illumination distribution of a scene. $\boldsymbol{n}(\boldsymbol{x})$ and $c_b(\lambda'')$ are the surface normal at the point $\boldsymbol{x}$ and the b-th band's spectral sensitivity of a camera respectively. It is reported that the brightness of a fluorescent component approximately obeys the Lambert model, *i.e.* is represented by the inner product between the surface normal and the light source direction (Sato et al., 2012; Treibitz et al., 2012).

We assume that the spectral sensitivity of a camera is narrow-band as is often assumed in color constancy algorithms. Namely, the spectral sensitivity is approximately represented by using the Dirac delta function; $c_b(\lambda'') \simeq \delta(\lambda'' - \lambda_b)$. Then, the integral with respect to λ'' in eq.(2) is represented as

$$\int c_b(\lambda'') e(\lambda'') d\lambda'' \simeq e(\lambda_b), \tag{3}$$

where we assume the peak value of the spectral sensitivity is 1 for the sake of simplicity.

The integral with respect to $\boldsymbol{\omega}$ in eq.(2) is the spectral irradiance $s(\boldsymbol{x},\lambda')$ due to incident light rays from various directions to the point $\boldsymbol{x}$ with the wavelength λ', and is defined by

$$s(\boldsymbol{x},\lambda') \equiv \int l(\boldsymbol{\omega},\lambda') \boldsymbol{\omega}^\top \boldsymbol{n}(\boldsymbol{x}) d\boldsymbol{\omega}. \tag{4}$$

We substitute eq.(4) into the integral with respect to λ' in eq.(2), and then approximately represent the integral by the summation with respect to the wavelengths of the 3 bands as

$$\int a(\lambda') s(\boldsymbol{x},\lambda') d\lambda' \simeq \sum_b a(\lambda_b) s(\boldsymbol{x},\lambda_b). \tag{5}$$

Substituting eq.(3) and eq.(5) into eq.(2), we obtain

$$f_b(\boldsymbol{x}) \simeq e(\lambda_b) \sum_{b'} a(\lambda_{b'}) s(\boldsymbol{x},\lambda_{b'}). \tag{6}$$

Therefore, the brightness of the fluorescent component is computed by the sum of the products between the 3-band absorption spectrum $a(\lambda_{b'})$ and the 3-band spectral irradiance $s(\boldsymbol{x},\lambda_{b'})$. The color of the fluorescent component is determined by the 3-band emission spectrum $e(\lambda_b)$.

2.3 Diffuse Reflection Model

According to the Lambert model, the diffuse reflection component is described as

$$\begin{aligned} r_b(\boldsymbol{x}) &= \int c_b(\lambda') \rho(\boldsymbol{x},\lambda') \left[\int l(\boldsymbol{\omega},\lambda') \boldsymbol{\omega}^\top \boldsymbol{n}(\boldsymbol{x}) d\boldsymbol{\omega} \right] d\lambda' \\ &= \int c_b(\lambda') \rho(\boldsymbol{x},\lambda') s(\boldsymbol{x},\lambda') d\lambda' \end{aligned} \tag{7}$$

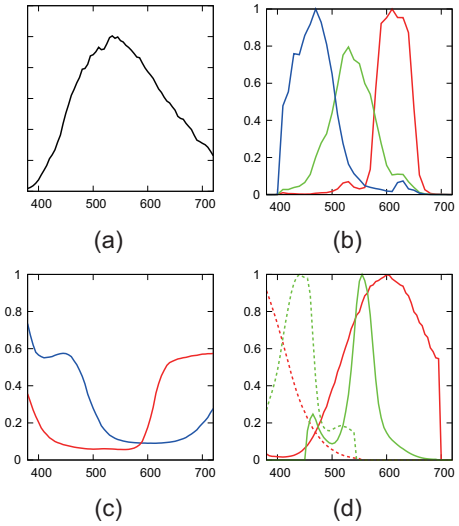

Figure 1: The spectral data for synthetic images. (a) the spectral intensity of a light source, (b) the spectral sensitivity of a camera, (c) the spectral reflectances of a reflective object (red: left, blue: right), and (d) the absorption and emission spectra of fluorescent materials (red: upper, green: lower).

Here, $\rho(\boldsymbol{x},\lambda')$ is the spectral reflectance at the point $\boldsymbol{x}$, and we use the definition of the spectral irradiance in eq.(4).

Assuming a narrow-band camera in a similar manner to the previous subsection, the diffuse reflection component is given by

$$r_b(\boldsymbol{x}) \simeq \rho(\boldsymbol{x},\lambda_b)s(\boldsymbol{x},\lambda_b). \quad (8)$$

Therefore, the diffuse reflection component is computed by the products between the 3-band spectral reflectance $\rho(\boldsymbol{x},\lambda_b)$ and the 3-band spectral irradiance $s(\boldsymbol{x},\lambda_b)$.

2.4 Adding Fluorescence

Our proposed method adds fluorescent components, whose absorption spectrum $a(\lambda')$ and emission spectrum $e(\lambda'')$ are specified by a user [1], to an object surface of interest in a single input image. Since both the 3-band absorption spectrum $a(\lambda_b)$ and the 3-band emission spectrum $e(\lambda'_b)$ in eq.(6) are given, the problem of computing photorealistic fluorescent components results in the estimation of the 3-band spectral irradiance $s(\boldsymbol{x},\lambda'_b)$.

On the other hand, the diffuse reflection components also depend on the 3-band spectral irradiance as shown in eq.(8), and therefore we can estimate the 3-band spectral irradiance from them. Specifically, we make use of intrinsic image decomposition without explicitly estimating the object's shape and the light sources illuminating it from the input image.

[1]The absorption and emission spectra can be selected from the McNamara dataset (McNamara et al., 2006).

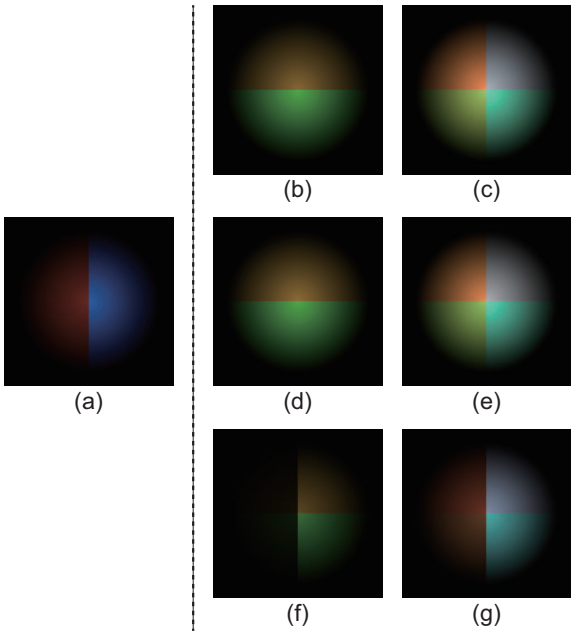

Figure 2: The experimental results using synthetic images. (a) the input image of a reflective object, (b) (d) (f) the fluorescent components, and (c) (e) (g) the result images, *i.e.* the fluorescent components are added to and the reflective components due to absorption are subtracted from the input image. The spectral rendering, our proposed method, and the naive method are used for (b) (c), (d) (e), and (f) (g) respectively.

Thus, our proposed method computes the fluorescent components from the user-provided absorption and emission spectra and the 3-band spectral irradiance estimated via intrinsic image decomposition. Specifically, our method replaces the pixel value $i_b(\boldsymbol{x})$ in the input image with $i'_b(\boldsymbol{x})$ computed as

$$i'_b(\boldsymbol{x}) = i_b(\boldsymbol{x}) + f_b(\boldsymbol{x}) - \rho(\boldsymbol{x},\lambda_b)a(\lambda_b)s(\boldsymbol{x},\lambda_b). \quad (9)$$

Here, the third term means that the reflective component decreases because a part of incident light rays is absorbed by the fluorescent material.

3 EXPERIMENTS

3.1 Synthetic Images

To confirm the effectiveness of our proposed method, we conducted qualitative and quantitative evaluation by using synthetic images. Specifically, we compared the following three methods for replacing a reflective object with a fluorescent one.

- **Spectral Rendering:** computes the fluorescent components according to eq.(2) under the condition that all the spectral data, *i.e.* the absorption spectrum $a(\lambda)$, the emission spectrum $e(\lambda)$, the spectral sensitivity $c_b(\lambda)$, and the spectral illumination distribution $l(\boldsymbol{x},\lambda)$ are given.
- **Our Proposed Method:** computes the fluorescent components according to eq.(6) under the condition that the 3-band absorption spectrum $a(\lambda_b)$, the 3-band emission spectrum $e(\lambda_b)$, and the 3-band spectral irradiance $s(\boldsymbol{x},\lambda_b)$ [2] are given.
- **Naive Method:** computes the fluorescent components according to eq.(6), but the pixel values of the input image are used instead of the 3-band spectral irradiance without using intrinsic image decomposition.

We synthesized the image of a sphere illuminated by a distant light source from the frontal direction. The spectral data used for synthesizing the input image are shown in Figure 1: (a) the spectral intensity of a light source, (b) the spectral sensitivity of a camera, (c) the spectral reflectances of a reflective object (red: left, blue: right), and (d) the absorption and emission spectra of fluorescent materials (red: upper, green: lower). Figure 2 shows (a) the input image of a reflective object, (b) (d) (f) the fluorescent components, and (c) (e) (g) the result images, *i.e.* the fluorescent components are added to and the reflective components due to absorption are subtracted from the input image. The spectral rendering, our proposed method, and the naive method are used for (b) (c), (d) (e), and (f) (g) respectively.

First, we can see that the fluorescent components and the result images computed by using (b) (c) the spectral rendering and (d) (e) our proposed method are similar to each other. The SSIM (Wang et al., 2003) and PSNR between (c) the result image of the spectral rendering and (e) that of our method are 0.971 and 40.41 respectively. Those results qualitatively and quantitatively show that our approximation represented by using the 3-band spectral irradiance works well.

Second, we can see that the fluorescent components and the result images computed by using (f) (g) the naive method are significantly different from those computed by using (b) (c) the spectral rendering. Specifically, (f) the fluorescent components are brighter at the area with bluish reflectance. This is because we specified fluorescent materials which absorb bluish light as shown in Figure 2 (d) and the naive method uses not the 3-band spectral irradiance but the pixel values of the input image without using intrinsic image decomposition. The SSIM and PSNR between (c) the result image of the spectral rendering and (g) that of the naive method are 0.791 and 20.64 respectively. Those results qualitatively and quantitatively show that the use of the 3-band spectral irradiance is important for computing photorealistic fluorescent components.

[2] In the experiments using synthetic images, we assume that the 3-band spectral irradiance is known.

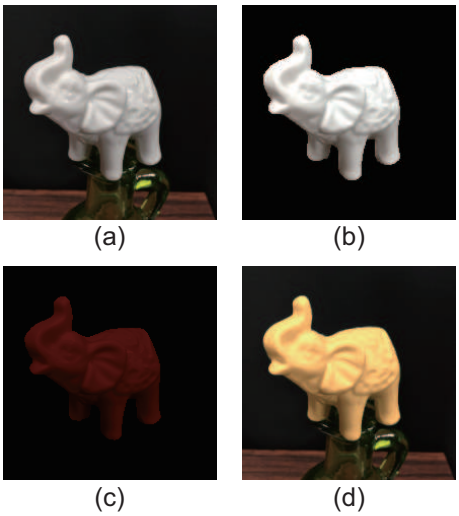

Figure 3: The experimental results using real images: an object with uniform reflectance. (a) the input image, (b) the 3-band spectral irradiance, (c) the fluorescent components, and (d) the result image computed by using our proposed method.

3.2 Real Images

To demonstrate the effectiveness of our proposed method for real images, we tested our method on three different conditions: (i) an object with uniform reflectance, (ii) an object with texture, and (iii) an object illuminated by an additional light source. In our experiments, we used SIRFS (Barron and Malik, 2015) for intrinsic image decomposition.

First, we tested an object with uniform reflectance as shown in Figure 3. Figure 3 shows (a) the input image, (b) the 3-band spectral irradiance, (c) the fluorescent components, and (d) the result image computed by using our proposed method. Here, we specified the 3-band absorption and emission spectra as $\boldsymbol{a} = (0,0,0.4)^\top$ and $\boldsymbol{e} = (0.8,0.2,0)^\top$ respectively. In other words, we assume that a fluorescent material absorbs bluish light and emits reddish light. We can see that (c) the fluorescent components and (d) the result image computed by using our method on the basis of the 3-band spectral irradiance are photometrically consistent with the input image; the object is illuminated mainly from the upper-right direction.

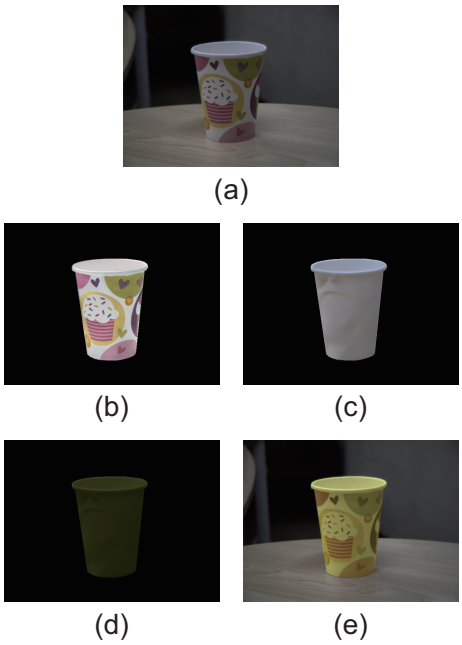

Figure 4: The experimental results using real images: an object with texture. (a) the input image, (b) the reflectance of the object, (c) the 3-band spectral irradiance, (d) the fluorescent components, and (e) the result image computed by using our proposed method.

Second, we tested an object with texture as shown in Figure 4. Figure 4 shows (a) the input image, (b) the reflectance of the object, (c) the 3-band spectral irradiance, (d) the fluorescent components, and (e) the result image computed by using our proposed method. The specified 3-band absorption and emission spectra are the same as the above. We can see that (d) the fluorescent components and (e) the result image computed by using our method are photometrically consistent with the input image; the object is illuminated almost uniform ambient light. Since our method makes use of the 3-band spectral irradiance estimated via intrinsic image decomposition, the computed fluorescent components are not contaminated by the texture on the object surface.

Third, we tested an object illuminated by an additional light source as shown in Figure 5. Figure 5 shows (a) the input image of an object illuminated by ambient light and (e) that illuminated by ambient light and an additional bluish light source from right. (b)/(f), (c)/(g), and (d)/(h) are the 3-band spectral irradiance, the fluorescent components, and the result images computed from (a)/(e) the corresponding input images by using our proposed method. The specified 3-band absorption and emission spectra are the same as the above. We can observe the photometrically consistent effects of the additional light source in (f), (g), and (h). Specifically, the 3-band spectral irradiance becomes bluish due to the bluish additional light source, and therefore the fluorescent components at the right areas become brighter since the specified fluorescent material absorbs bluish light.

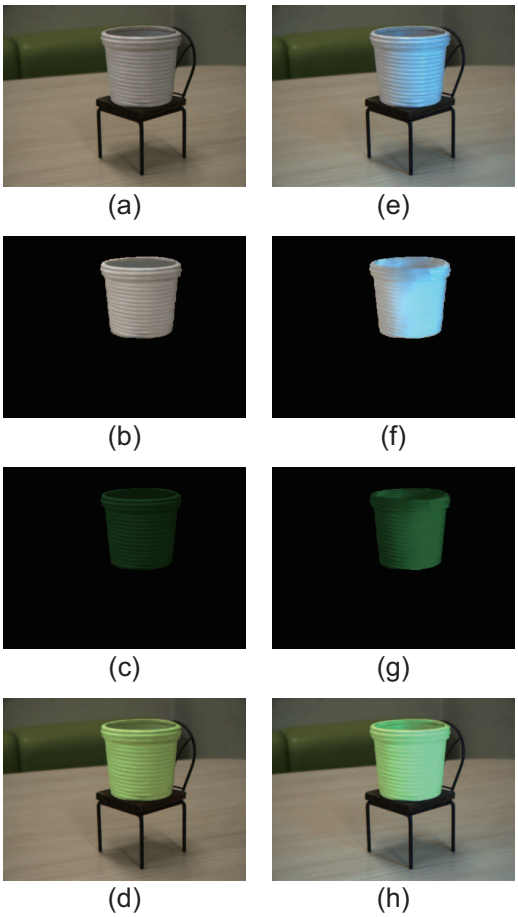

Figure 5: The experimental results using real images: an additional light source. (a) the input image of an object illuminated by ambient light and (e) that illuminated by ambient light and an additional bluish light source from right. (b)/(f), (c)/(g), and (d)/(h) are the 3-band spectral irradiance, the fluorescent components, and the result images computed from (a)/(e) the corresponding input images by using our proposed method.

4 CONCLUSION

In this paper, we proposed a method for making reflective objects in a single input image fluorescent by adding photorealistic fluorescent components to the objects of interest. Specifically, we show that photometrically consistent fluorescent components can approximately be represented by using the 3-band spectral irradiance on the surface of a reflective object, and then compute the fluorescent components on the ba-

sis of intrinsic image decomposition without explicitly estimating the object's shape and the light sources illuminating it from the input image. We conducted a number of experiments using both synthetic and real images, and confirmed that our proposed method is effective for making reflective objects fluorescent. Taking specular reflection and inter-reflection components in an input image into consideration is one of the future directions of this study.

ACKNOWLEDGMENTS

This work was partially supported by JSPS KAKENHI Grant Numbers JP18H05011 and JP17H01766.

REFERENCES

Barnard, K. (1999). Color constancy with fluorescent surfaces. In *Proc. CIC1999*, pages 257–261.

Barron, J. and Malik, J. (2015). Shape, illumination, and reflectance from shading. *IEEE TPAMI*, 38(7):1670–1687.

Fu, Y., Lam, A., Sato, I., Okabe, T., and Sato, Y. (2016a). Reflectance and fluorescence spectral recovery via actively lit RGB images. *IEEE TPAMI*, 38(7):1313–1326.

Fu, Y., Lam, A., Sato, I., Okabe, T., and Sato, Y. (2016b). Separating reflective and fluorescent components using high frequency illumination in the spectral domain. *IEEE TPAMI*, 38(5):965–978.

Khan, E., Reinhard, E., Fleming, R., and Bülthoff, H. (2006). Image-based material editing. In *Proc. ACM SIGGRAPH2006*, pages 654–663.

Koyamatsu, K., Hidaka, D., Okabe, T., and Lensch, H. (2019). Reflective and fluorescent separation under narrow-band illumination. In *Proc. IEEE CVPR2019*, pages 7577–7585.

Liu, G., Ceylan, D., Yumer, E., Yang, J., and Lien, J.-M. (2017). Material editing using a physically based rendering network. In *Proc. IEEE ICCV2017*, pages 2261–2269.

McNamara, G., Gupta, A., Reynaert, J., Coates, T., and Boswell, C. (2006). Spectral imaging microscopy web sites and data. *Cytometry Part A*, 69A(8):863–871.

Sato, I., Okabe, T., and Sato, Y. (2012). Bispectral photometric stereo based on fluorescence. In *Proc. IEEE CVPR2012*, pages 270–277.

Tappen, M., Freeman, W., and Adelson, E. (2005). Recovering intrinsic images from a single image. *IEEE TPAMI*, 27(9):1459–1472.

Treibitz, T., Murez, Z., Mitchell, G., and Kriegman, D. (2012). Shape from fluorescence. In *Proc. ECCV2012*, pages 292–306.

Wang, Z., Bovik, A., Sheikh, H., and Simoncelli, E. (2003). Image quality assessment: from error visibility to structural similarity. *IEEE TIP*, 13(4):600–612.

Zhang, C. and Sato, I. (2013). Image-based separation of reflective and fluorescent components using illumination variant and invariant color. *IEEE TPAMI*, 35(12):2866–2877.